

Spatial analysis of global urban extent from DMSP-OLS night lights

Christopher Small^{a,*}, Francesca Pozzi^b, C. D. Elvidge^c

^aLamont Doherty Earth Obs., Columbia University, Palisades, NY 10964, USA

^bCIESIN, Columbia University, Palisades, NY 10964, USA

^cNOAA National Geophysical Data Center, 325 Broadway, Boulder, CO 80303, USA

Received 2 September 2004; received in revised form 27 January 2005; accepted 1 February 2005

Abstract

Previous studies of DMSP-OLS stable night lights have shown encouraging agreement between temporally stable lighted areas and various definitions of urban extent. However, these studies have also highlighted an inconsistent relationship between the actual lighted area and the boundaries of the urban areas considered. Applying detection frequency thresholds can reduce the spatial overextent of lighted area (“blooming”) but thresholding also attenuates large numbers of smaller lights and significantly reduces the information content of the night lights datasets. Spatial analysis of the widely used 1994/1995 stable lights data and the newly released 1992/1993 and 2000 stable lights datasets quantifies the tradeoff between blooming and attenuation of smaller lights. For the 1992/1993 and 2000 datasets, a 14% detection threshold significantly reduces blooming around large settlements without attenuating many individual small settlements. The corresponding threshold for the 1994/1995 dataset is 10%. The size–frequency distributions of each dataset retain consistent shapes for increasing thresholds while the size–area distributions suggest a quasi-uniform distribution of lighted area with individual settlement size between 10 and 1000 km equivalent diameter. Conurbations larger than 80 km diameter account for <1% of all settlements observed but account for about half the total lighted area worldwide. Area/perimeter distributions indicate that conurbations become increasingly dendritic as they grow larger. Comparison of lighted area with built area estimates from Landsat imagery of 17 cities shows that lighted areas are consistently larger than even maximum estimates of built areas for almost all cities in every light dataset. Thresholds >90% can often reconcile lighted area with built area in the 1994/1995 dataset but there is not one threshold that works for a majority of the 17 cities considered. Even 100% thresholds significantly overestimate built area for the 1992/1993 and 2000 datasets. Comparison of lighted area with blooming extent for 10 lighted islands suggests a linear proportionality of 1.25 of lighted to built diameter and an additive bias of 2.7 km. While more extensive analyses are needed, a linear relationship would be consistent with a physical model for atmospheric scattering combined with a random geolocation error. A Gaussian detection probability model is consistent with an observed sigmoid decrease of detection frequency for settlements <10 km diameter. Taken together, these observations could provide the basis for a scale-dependent blooming correction procedure that simultaneously reduces geolocation error and scattering induced blooming.

© 2005 Published by Elsevier Inc.

Keywords: Spatial analysis; Global urban land cover; DMSP-OLS night lights; Landsat

1. Introduction

Satellite imaging of stable anthropogenic lights provides an accurate, economical and straightforward way to map the global distribution of urban areas. Urban areas account for a small fraction of Earth’s surface area but exert a disproportional

influence on their surroundings in terms of mass, energy and resource fluxes. The spatial distribution and size–frequency characteristics of the global urban network have important implications for disciplines ranging from economics (e.g. Fujita et al., 1999; Krugman, 1996) to ecology (e.g. Cincotta et al., 2000) to astronomy (Cinzano et al., 2001a,b). In spite of its importance, accurate representations of global urban extent are difficult to derive from administrative definitions (Balk et al., 2004). While there are many irreconcilable administrative definitions of urban

* Corresponding author.

E-mail address: small@LDEO.columbia.edu (C. Small).

extent currently in use, physical measurements of lighted area can provide a self-consistent metric on which to base comparative analyses of urban extent. Temporally stable upwelling radiance is unique to anthropogenic land use and can be measured by the Defense Meteorological Satellite Program (DMSP) Operational Linescan System (OLS) system (Croft, 1978). However, there are caveats inherent to this characterization of urban extent. Specifically, the area and intensity of illumination are known to vary significantly with energy availability, economic development and density of settlement (Elvidge et al., 1997; Sutton et al., 1997). Some of these variations have been quantified at national scales but direct comparisons of urban extent and lighted area have only been done for a few cities.

Previous analyses have revealed a consistent disparity between various spatial measures of urban extent and the spatial extent of lighted areas in the night lights datasets (Welch, 1980; Welch & Zupko, 1980). Specifically, the lighted areas detected by the OLS are consistently larger than the geographic extents of the settlements they are associated with. The larger spatial extent of lighted area, relative to developed land area, is sometimes referred to as “blooming”. The blooming is the result of three primary phenomena, including: (1) the relatively coarse spatial resolution of the OLS sensor and the detection of diffuse and scattered light over areas containing no light source, (2) large overlap in the footprints of adjacent OLS pixels, and (3) the accumulation of geolocation errors in the compositing process (Elvidge et al., 2004). In the context of this study, blooming refers to spurious indication of light in a location that does not contain a light source.

In order to offset the blooming effect, Imhoff et al. (1997) proposed using a threshold of 89% detection frequency to eliminate less frequently detected lighted pixels at the peripheries of large urban areas. Imposing a detection frequency threshold effectively shrinks the lighted areas so they are more consistent with administrative definitions of urban extent. The drawback associated with detection frequency thresholds is that they also attenuate large numbers of smaller, less frequently detected settlements. The 89% threshold proposed by Imhoff et al. (1997) was derived from an average of 85%, 89% and 94% thresholds determined for the cities of Chicago, Sacramento and Miami, respectively. At the state level, the 89% threshold significantly increased the correlation (from 0.87 to 0.97) between lighted area and US Census-defined urban areas, despite the numerous caveats of using administrative boundaries that were discussed by Imhoff et al. (1997). In a subsequent analysis, Sutton et al. (2001) obtained a correlation of 0.68 between $\ln(\text{lighted area})$ and $\ln(\text{population})$ when using a threshold of 80%. These authors recognized the limitations of using a single threshold for a global analysis and also used a combination of 40%, 80% and 90% thresholds for a global analysis of lighted area and aggregate population (Sutton et al., 2001). In another recent study (Henderson et al., 2003),

the authors were able to avoid some of the confounding factors associated with administrative (cadastral) delineations of urban extent by comparing lighted area with urban boundaries derived from Landsat TM imagery. Using Supervised Maximum Likelihood classifications of Beijing, Lhasa and San Francisco, these authors obtained optimum thresholds of 97%, 88% and 92%, respectively. They also found that these thresholds resulted in significant lateral shifts between the lighted area and the Landsat-derived urban boundary. These studies all suggest that it may be possible to obtain reasonable agreement between lighted area and various measures of city size but these studies also reveal significant variability in the relationship between lighted area and different definitions of urban extent. All of these studies have emphasized the need for more extensive analyses of lighted area, detection thresholds and urban extent.

The objectives of this analysis are to quantify the global size–frequency distribution of stable contiguous lighted areas and to investigate the correspondence between the spatial extent of urban land use and lighted area. In the context of this study, we refer to all developed non-agricultural land (i.e. urban, suburban, exurban) as “urban”. We conduct a series of comparative analyses of the 1994/1995 light dataset used in previous studies and the new 2000 and 1992/1993 datasets recently released by Elvidge et al. (2004). Because previous studies have highlighted the importance of detection frequency thresholds on lighted area, we first quantify the dependence of lighted area and size–frequency distributions on detection frequency threshold. Because the light data provide a unique measure of urban morphology across a wide range of sizes, we also quantify the shape distributions as area/perimeter ratios. In the second part of the analysis, we compare lighted areas with Landsat-derived estimates of urban land use for 17 cities worldwide. We also compare the extent of blooming to lighted area for 10 islands of varying size. The objective of these comparisons is to quantify the spatial overextent of lighted area for each dataset for different detection frequency thresholds to determine if there is a consistent relationship that can be used to correct for the spatial overextent. The overall purpose of this analysis is to quantify the systematics of the global distributions of size, shape and frequency of detection for different OLS night lights datasets and to illustrate their correspondence to other physical measures of urban land use. By quantifying the physical consistencies of the lights data, we hope to facilitate future analyses of the non-physical (i.e. socio-economic, cultural, political) determinants of urban extent and stable radiance.

2. Data

The 1994–1995 nighttime lights dataset is a cloud-free composite of OLS data collected between October 1,

1994 and March 31, 1995 under low moon conditions (Elvidge et al., 2004). The processing involved the manual selection of usable orbital segment, semi-automatic cloud detection, and filtering to detect lights relative to the local background. The basic algorithms have been described in Elvidge et al. (1997). The

products used in this analysis are percent frequency of detection images in which values between 0 and 100 indicate the percent frequency of light detection within the set of cloud-free observations over the duration of the observations. The lights were separated into four categories (fires, gas flares, fishing boats, and human settle-

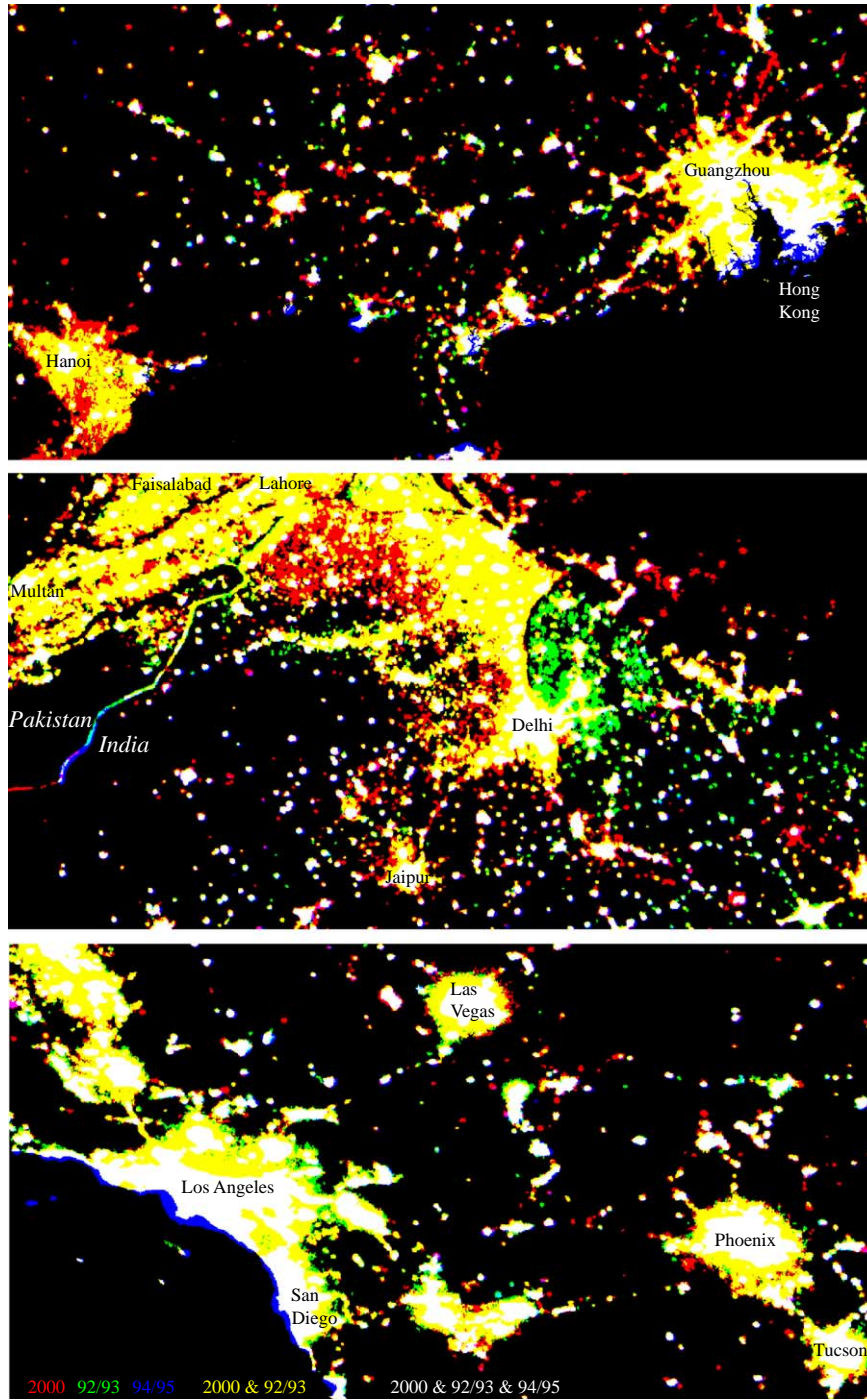


Fig. 1. Night light composites. Each dataset is represented by a primary color (R/G/B) while areas lighted in two or three datasets are represented as additive colors (white & yellow). The original 94/95 dataset resolves urban cores and moderate sized settlements while the newer datasets resolve smaller settlements and more diffuse lights at settlement peripheries. The 94/95 dataset is not masked at the coastlines so the effect of “blooming” over water is apparent as blue fringes on coastal cities.

ments) through visual interpretation of the percent frequency image.

The 1992–1993 and 2000 nighttime lights datasets are cloud-free composites processed specifically with the objective of change detection. The production was considerably more automated than the methods used for the 1994/1995 product. Data from 2 years (1992 and 1993) were used for the first time period due to major temporal gaps present at the start of the archive in mid-1992. The processing included automatic cloud detection and a modified light detection algorithm designed to capture dim lighting. Products include the percent frequency (same as 1994–1995 product) and the average digital number of the detected lights. Fires were separated from human settlements based on their high brightness levels and low persistence. The products are not radiance calibrated due to the lack of on-board calibration and uncertainty in the gain settings.

For consistency with the widely used 1994/1995 detection frequency data, we calculated percent frequency of detection for the 1992/1993 and 2000 datasets. Percent frequency of detection is calculated as 100 times the ratio of the cloud-free light count to the cloud-free coverage count. These three light datasets can be compared directly in the form of a three-color composite in which the 2000, 1992/1993 and 1994/1995 data are assigned to the red, green and blue channels respectively (Fig. 1). In this format, unlighted areas are black while the primary colors show areas represented in only one of the three datasets. Yellow areas highlight the greater spatial extent of the 2000 and 1992/1993 datasets into areas not illuminated in the 1994/1995 dataset. Throughout the analysis we refer to clusters of adjacent lighted pixels as contiguous lighted areas. We assume that spatial distributions of these lighted areas reflect characteristics of a detectable subset of human settlements.

3. Spatial analysis

3.1. Polygons, centroids and threshold area estimation

In order to quantify the dependence of lighted area and size–frequency distributions on detection frequency threshold, we calculated the number of contiguous light polygons, their area, perimeter, and latitude and longitude of their centroids for each dataset (1992/1993, 1994/1995 and 2000) at different thresholds. Using ArcInfo commands and ArcView scripts, we calculated the number of light polygons and their area and perimeter for each threshold at 10% intervals between 0% and 100% frequency, and at 2% intervals between 0% and 30% frequency. The latitude and longitude coordinates were then assigned to the centroids of each contiguous lighted area. To quantify the correspondence between size and frequency of detection, we calculated the detection frequency at the centroid of each polygon at 10% intervals. This was done by combining the original

light frequency datasets with the file containing the latitude and longitude coordinates of the centroids of the contiguous light polygons. This way, each contiguous lighted area is assigned a detection frequency value corresponding to its centroid. Because most people find linear distance more intuitive than area, we generally represent the size of each irregularly shaped contiguous lighted area as equivalent circular diameter defined as $2 \times \text{Sqrt}(\text{Area}/\pi)$.

3.2. Thresholds and size–frequency distributions

Increasing the frequency of detection threshold results in both fragmentation and attenuation of contiguous lighted areas. The changes in the total lighted area and number of contiguous lights with increasing detection threshold shown in Fig. 2 illustrate the combined effects of fragmentation and attenuation. Attenuation occurs when smaller, less frequently detected lights fall below the detection frequency threshold and disappear from the threshold-limited map. Increasing the frequency of detection threshold also reduces the lighted area of larger settlements as the lower frequency pixels at the peripheries are exceeded by the threshold value. Fragmentation occurs when a contiguous lighted area subdivides into smaller areas as the detection threshold increases. This corresponds to lighted areas in which two or more centers of high detection frequency are joined into a larger contiguous

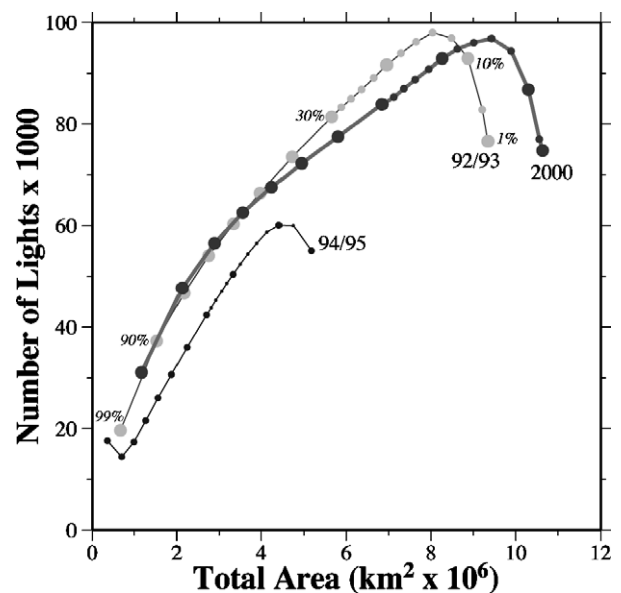


Fig. 2. Change in lighted area and number of contiguous lights for different detection frequency thresholds. As thresholds increase from $\geq 1\%$ to $\geq 99\%$ the total lighted area diminishes monotonically but the number of contiguous lights initially increases as large conurbations fragment. As thresholds increase further the number of lights diminishes as greater numbers of smaller, less frequently detected, lights are attenuated. A 14% detection frequency threshold results in the maximum number of individual lights for the 2000 and 1992/1993 datasets while a 10% threshold maximizes the number of lights in the 1994/1995 dataset. Note that the newer 2000 and 1992/1993 datasets detect about twice the number of lights and lighted area as the older 1994/1995 dataset.

light by lower frequency pixels in the area between the higher frequency centers. Large conurbations are actually composed of multiple bright, frequently detected urban centers for which peripheral blooming overlaps, plus dim lighting detected outside of traditional urban boundaries. Increasing the detection frequency threshold attenuates the blooming thereby causing the larger contiguous lighted area to fragment into smaller centers of higher detection frequency. Fig. 2 shows how the number of contiguous lights initially increases as the frequency detection thresh-

old goes from 0 to 14% (10% for the 1994/1995 dataset) but then decreases at higher thresholds. The decrease occurs as the rate of attenuation exceeds the rate of fragmentation.

Comparison of size–frequency distributions and size–area distributions illustrates the effect of detection frequency thresholds on the number of contiguous lights and total lighted area. The size–frequency distributions in Fig. 3 (left column) show the simultaneous decrease in number and size of contiguous lights with increasing threshold. The peaks of

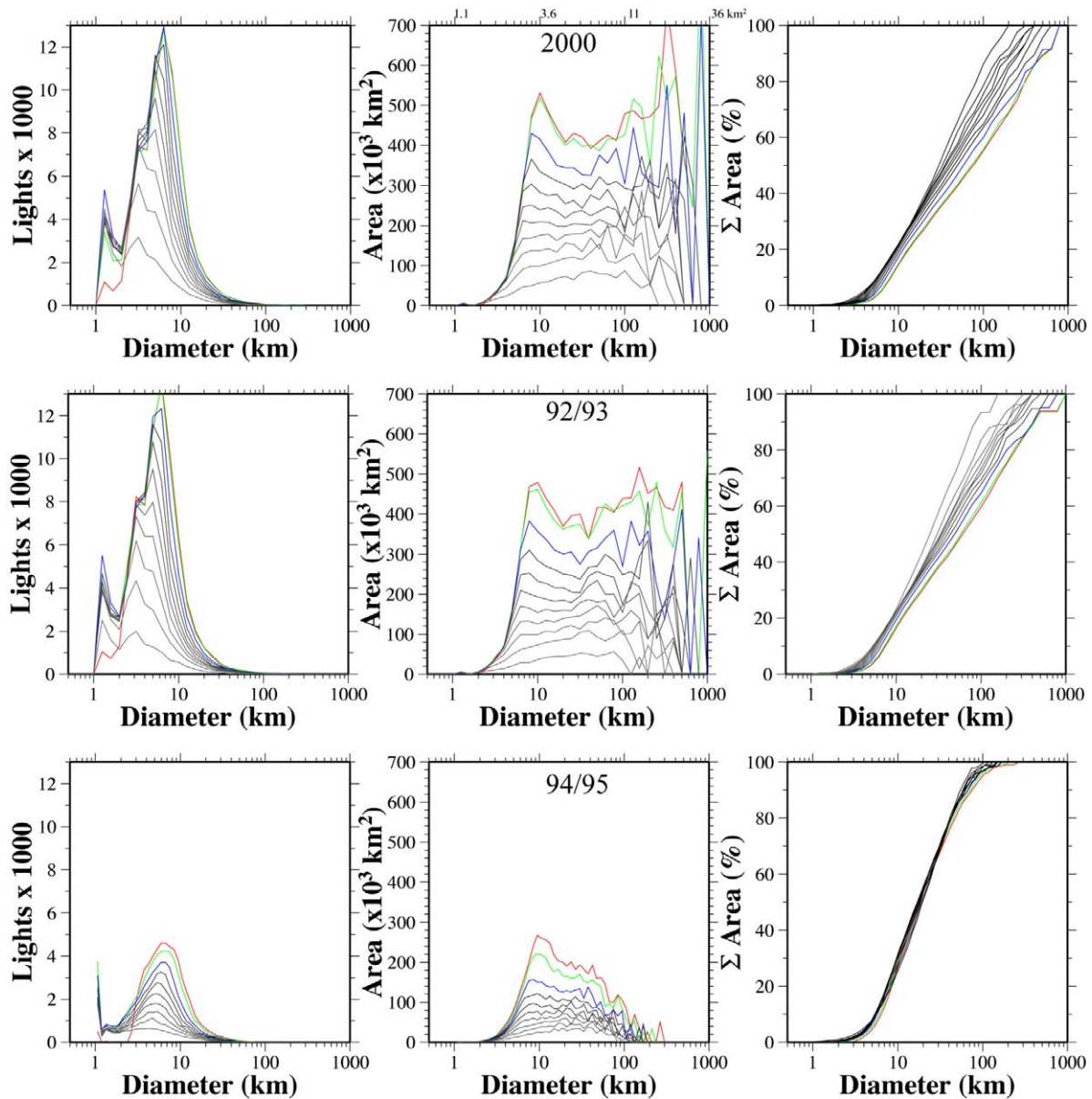


Fig. 3. Distributions of numbers and areas of lights as functions of equivalent circular diameter for different frequency detection thresholds. Each curve shows the histogram (cumulative in the right column) corresponding to an incremental 10% frequency detection threshold. As the thresholds increase from $\geq 1\%$ to $\geq 99\%$ the number and area of lights change (as shown in Fig. 2) and the histograms generally shrink. The quasi-parabolic decrease in the number of detected lights with increasing diameter results in nearly uniform distributions of lighted area for the 2000 and 1992/1993 datasets while the distribution becomes increasingly uniform with increasing threshold for the 1994/1995 dataset. The vast majority of individual contiguous lights are < 80 km in diameter but the minority ($< 1\%$) of conurbations corresponding to those > 80 km accounts for about half of the world's lighted urban area.

the size–frequency distributions diminish rapidly while the modal (peak) diameter shifts from 6.5 to 3.5 km diameter. The size–area distributions show the total lighted area for each size range of equivalent diameters. The quasi-uniform size–area distributions (center column) diminish almost evenly and the slight mode at 10 km diameter gradually disappears. The cumulative area distributions (right column) show a corresponding shift to smaller median and maximum diameters with increasing threshold. These distributions indicate that while the vast majority (>99%) of individual contiguous lighted areas are less than 80 km in equivalent diameter, the small minority (<1%) that are larger account

for approximately half of the total lighted area worldwide. These correspond to large conurbations.

Smaller lighted areas are detected less frequently than larger contiguous areas. Comparing the equivalent diameter of each contiguous lighted area to its frequency of detection (at its centroid) illustrates the correspondence between size (diameter) and frequency of detection. Fig. 4 (left column) shows a rapid increase in detection frequency as diameters increase from 2 to 10 km. The lights always detected tend to be larger than ~8 km diameter in the 1992/1993 and 2000 datasets and larger than 10 km in the 1994/1995 dataset. Distributions of numbers of contiguous

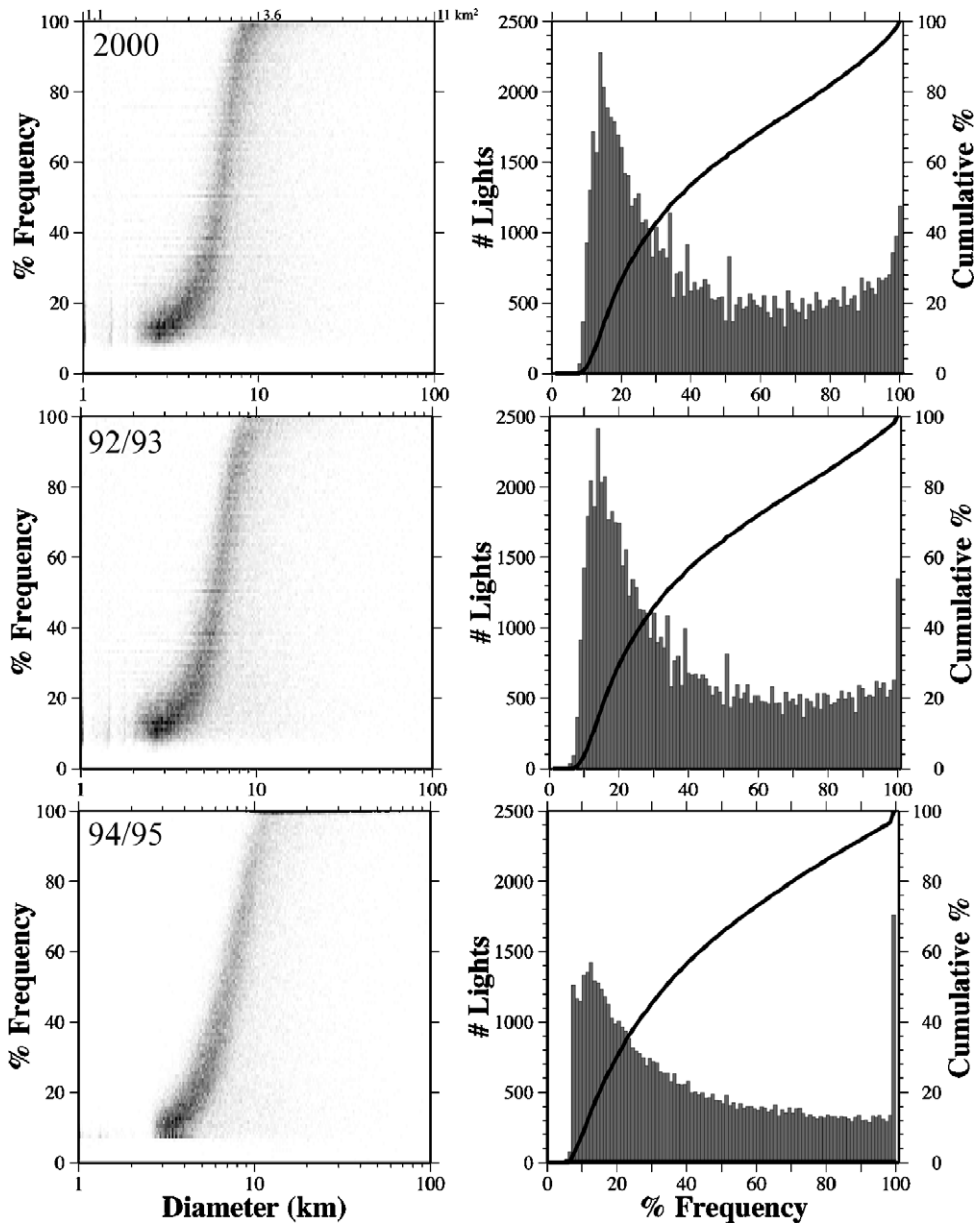


Fig. 4. Bivariate distributions of individual contiguous lights as functions of equivalent circular diameter and % frequency of detection (left) and corresponding marginal distributions for frequency (right). Darker grays (on left) correspond to exponentially greater lighted area. In all three datasets, the frequency of detection increases sigmoidally with diameter for lights less than ~10 km and is consistently high for lights larger than 10 km. The marginal distributions (bivariates summed over all diameters) show a distinct mode corresponding to lights that are always detected (100%).

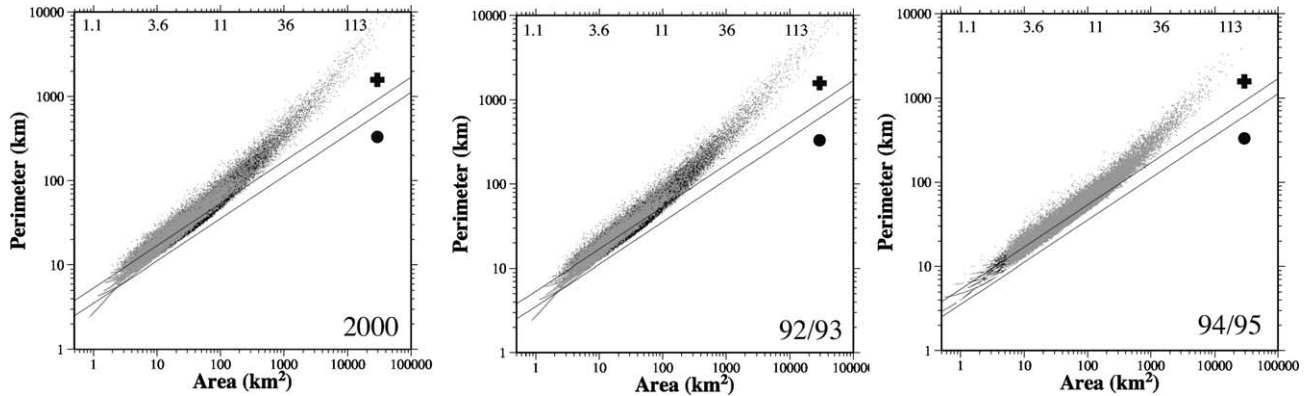


Fig. 5. Area/Perimeter distributions of contiguous lighted areas. Each point corresponds to a distinct contiguous lighted area. Gray points show lights resulting from the $\geq 99\%$ detection frequency threshold while black points show the distribution corresponding to the $\geq 1\%$ threshold. Equivalent circular diameters (in km) are shown along the top axes. Diagonal lines show the area/perimeter ratios corresponding to circles (lower) and equilateral crosses. The upward curvature of the distributions results from increasingly tortuous boundaries of larger conurbations.

lights as a function of frequency of detection (Fig. 4, right column) illustrate bimodal frequency distributions in which several thousands of lights are almost always detected while much larger numbers of lights are detected less than 20% of the time. The former correspond to large urban areas while the latter are generally less than 10 km in diameter.

3.3. Area/perimeter distributions

Area/Perimeter ratios are often used to quantify the planform shape of urban areas (e.g. Batty and Longley, 1996). Circular cities are maximally compact with a minimal ratios while dendritic cities with more tortuous boundaries have higher ratios. Area/Perimeter plots (Fig. 5) for the city lights datasets indicate that larger lighted areas have increasingly convoluted boundaries while the smallest lights approach circular ratios. True circular ratios are never attained because the lights are represented as aggregates of quadrilateral pixels. The upward curvature of the area–perimeter distributions reveals increasingly higher ratios for lights larger than ~ 10 km diameter. A few of the smallest lights in the 1992/1993 and 2000 datasets have infeasibly low (sub-circular) ratios as a result of projection induced error in the perimeter calculation.

4. Comparison with Landsat ETM+

4.1. Built area estimation from Landsat ETM+

The Landsat TM and ETM+ sensors clearly resolve spectral differences between developed urban land cover and undeveloped non-anthropogenic land covers. The correspondence between lighted area and urban land use can be quantified using Landsat imagery. Although thematic classification of urban land use has traditionally been rather subjective and error-prone, estimates of urban extent based on spectral heterogeneity offer an alternative means of

comparing built area and lighted area. Spectral Mixture Analysis (SMA) provides a physical basis on which to quantify the spectral characteristics of diverse mosaics of land covers and distinguish spectrally heterogeneous urban areas from more spectrally homogeneous non-urban land covers. Comparative spectral mixture analyses of Landsat and Ikonos imagery for a variety of cities worldwide indicate that urban and periurban land use can be distinguished on the basis of spectral heterogeneity at scales of 15 to 50 m (Small, 2002, 2003, 2005). Despite variability in spectral characteristics among and within cities, the comparative analyses indicate that spectral heterogeneity can be used to provide estimates of urban extent in places where surrounding non-anthropogenic land cover is spectrally distinct (Small, 2002). One benefit of defining urban extent on the basis of spectral heterogeneity is the ability to generate a range of verifiable extent estimates (ranging from minimum to maximum) that encompasses a range of different definitions of the urban area. This eliminates the considerable ambiguity resulting from varying administrative and political definitions of urban areas. The data and methodology used in the present analysis are based on the analysis of the spectral properties of 28 diverse urban areas imaged by Landsat ETM+ is given by Small (2005).

Landsat ETM+ imagery was selected from the quasi-random collection analysed by Small (2005). The selection is quasi-random in the sense that it was based on availability of cloud-free imagery in the ETM+ archive at the Global Land Cover Facility at the University of Maryland. The cities used for comparison with the nighttime lights data were chosen on the basis of size, diversity, availability of validation data and the ability of the heterogeneity analysis to accurately define consistent maximum and minimum urban extents from the Landsat data. Each Landsat subscene is 30×30 km and was chosen to encompass the city center as well as a diversity of surrounding non-urban land covers. All ETM+ images were acquired between 1999 and 2002.

For each ETM+ subscene, a suite of five estimates of urban extent was generated on the basis of spectral

heterogeneity as illustrated by Small (2005). Each suite ranges from minimal to maximal urban extent as determined by the degree of spectral heterogeneity and comparison with conventional administrative maps of urban areas for individual cities in the 2000 Oxford World Atlas. While the latter criteria is admittedly ad hoc, it does provide a more consistent metric than those generally used in thematic urban classifications (which assume spectral homogeneity) and is a far more consistent urban definition than could be obtained from administrative maps alone. The spectral definition is more consistent because it is based on the fine scale heterogeneity common to all urban mosaics rather than administrative boundaries that do not necessarily contain the entire developed area and generally contain unlighted areas like parks and water bodies. By comparing lighted extent to both maximal and minimal extents of urban land cover derived from Landsat imagery, the comparison is guaranteed to encompass all reasonable configurations of urban land use that might contribute to the lighted area as well as any physical definition of urban extent. For brevity, the Landsat-derived estimates of urban extent are henceforth referred to

as built area estimates. The maximum–minimum range of built area estimates for each city indicates the uncertainty in the estimation process. It is encouraging that the range of areas for each city is generally small compared to the average size of the city. The estimate ranges for each city are also small (<100 km²) compared to the total range of city sizes (<100 km² to >500 km²).

4.2. Comparison of lighted areas with ETM+ built areas

Qualitative comparison of lighted extent with Landsat-derived estimates of urban extent suggests that the 1992/1993 and 2000 light datasets overestimate the built area to a greater extent than does the 1994/1995 dataset. Fig. 6 shows a comparison of ETM+ false color imagery, minimum and maximum urban extent estimates and all three light datasets for Hanoi, Vietnam. The white areas correspond to the maximal estimate of built area within the lighted area while the cyan (green+blue) areas show the minimal estimate outside the lighted area and the green areas show the maximum estimate outside the lighted area. Both the 1994/

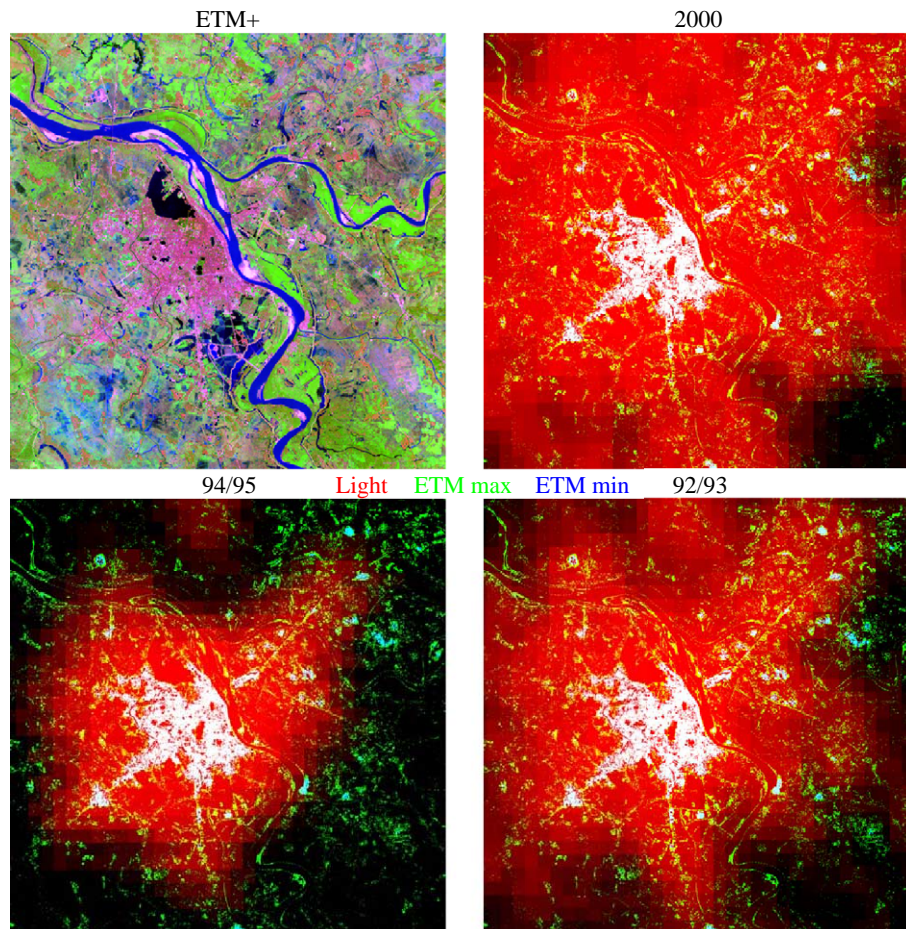


Fig. 6. Comparison of Landsat-derived built area with lighted areas for Hanoi Vietnam. Landsat ETM+ false color composite (R/G/B=7/4/2) shows a mosaic of built area, water, agriculture and fallow fields. The lighted and built area color composites (R/G/B=Light area/Maximum built area/Minimum built area) show variations of lighted area for different lights datasets and the range of distributions of built area estimates. While indicates minimum built area within the lighted area while yellow shows the maximum extent of built area within the lighted area. Green and cyan indicate maximum and minimum built area (respectively) outside the lighted area.

1995 and 1992/1993 light datasets provide a reasonable representation of the urban core and primary radial development corridors. The 2000 dataset significantly overestimates even the maximum extent of built area from the ETM+ imagery. Numerous agricultural and forested areas are depicted with high light detection frequency in the 2000 data. This is the case for all 17 cities used in this study. In many of these cities, the 1992/1993 lighted area is also significantly larger than even the maximum estimate of built area. The 1994/1995 lighted areas are much closer to the

Landsat-derived estimates but still generally overestimate the built area as shown in Fig. 7. It is encouraging, however, that the overall shapes of the most densely built up areas depicted in the Landsat estimates are also seen in the 1994/1995 lighted areas. Shanghai is not shown in Fig. 7 because the lighted area completely filled the 30 × 30-km image.

Quantitative comparisons of lighted extent with Landsat-derived estimates of urban extent confirm that the 1992/1993 and 2000 light datasets do indeed overestimate the built area to a much greater extent than does the 1994/1995

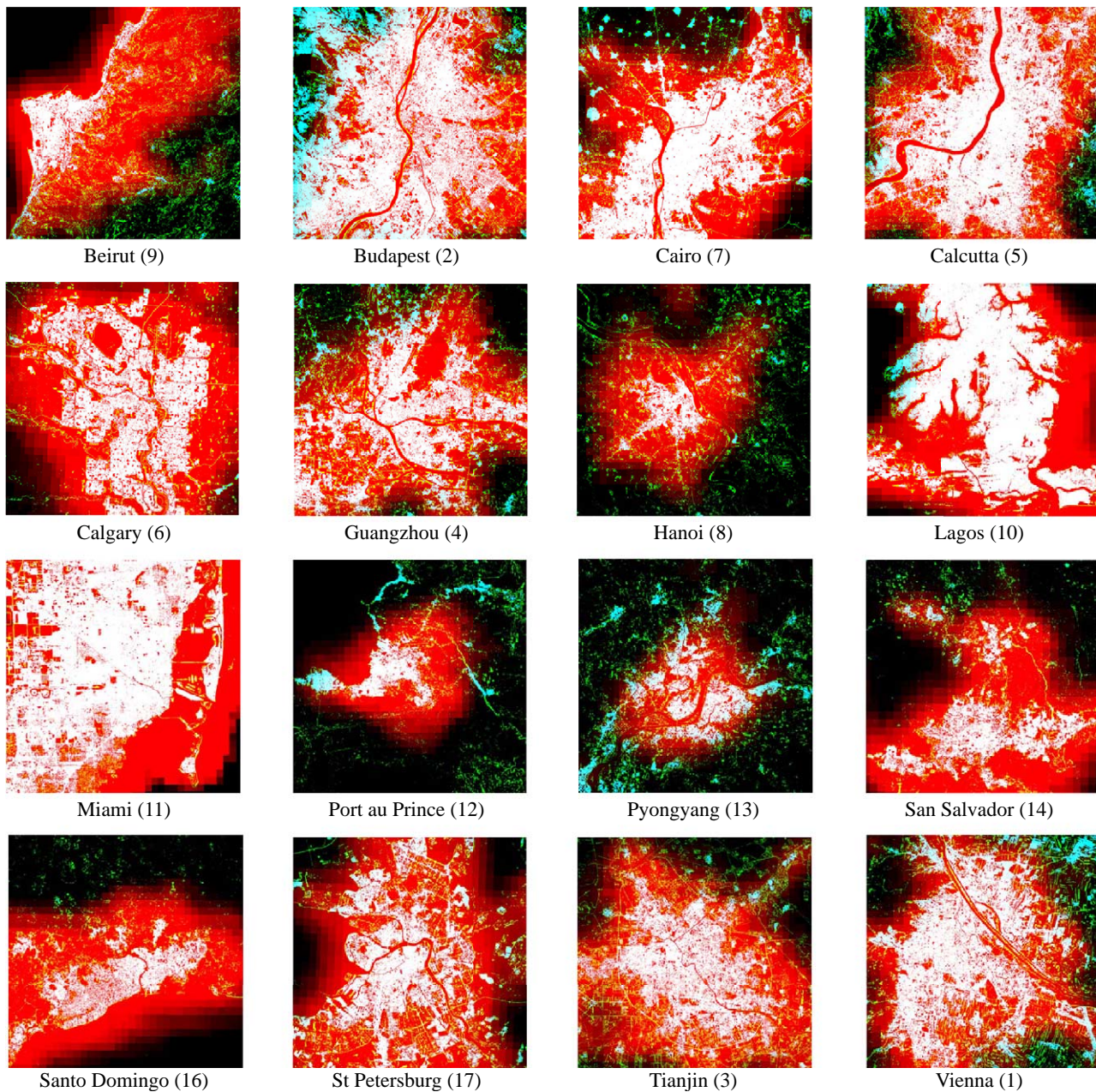


Fig. 7. Comparison of 94/95 lighted areas and Landsat-derived built extents for 16 urban areas. Color coding as in Fig. 6. Fragmentation of urban cores (white) generally results from undeveloped areas of intraurban water or vegetation that do not have the characteristic spectral heterogeneity on which the built area classification is based. The numbers correspond to the points in Fig. 8.

dataset. For each city, we calculated the total area of the maximum and minimum extents estimated from the ETM+ data and the total lighted area for each detection threshold. The curves in Fig. 8 show the decrease of lighted area with increasing threshold (left) with ETM+ built areas superimposed at the corresponding threshold where the lighted area equals the average built area. The shapes of the curves indicate that most cities have lighted areas that are dominated by high detection frequencies with thin peripheries of lower frequencies (consistently high areas with precipitous drops at high frequencies) while a few have

smaller frequently detected core areas with broad peripheries of diminishing detection frequency (more uniform decrease in area with frequency). Note that in almost every case the lighted area most closely matching the built area estimate occurs at >90% detection frequency. This is consistent with the results of previous studies although there is no single threshold that produces consistent agreement for a majority of the cities considered. Plotting lighted area ranges against built area ranges (Fig. 8 right) clearly shows the degree to which the 1992/1993 and 2000 lighted areas overestimate the built areas. In almost every case, the

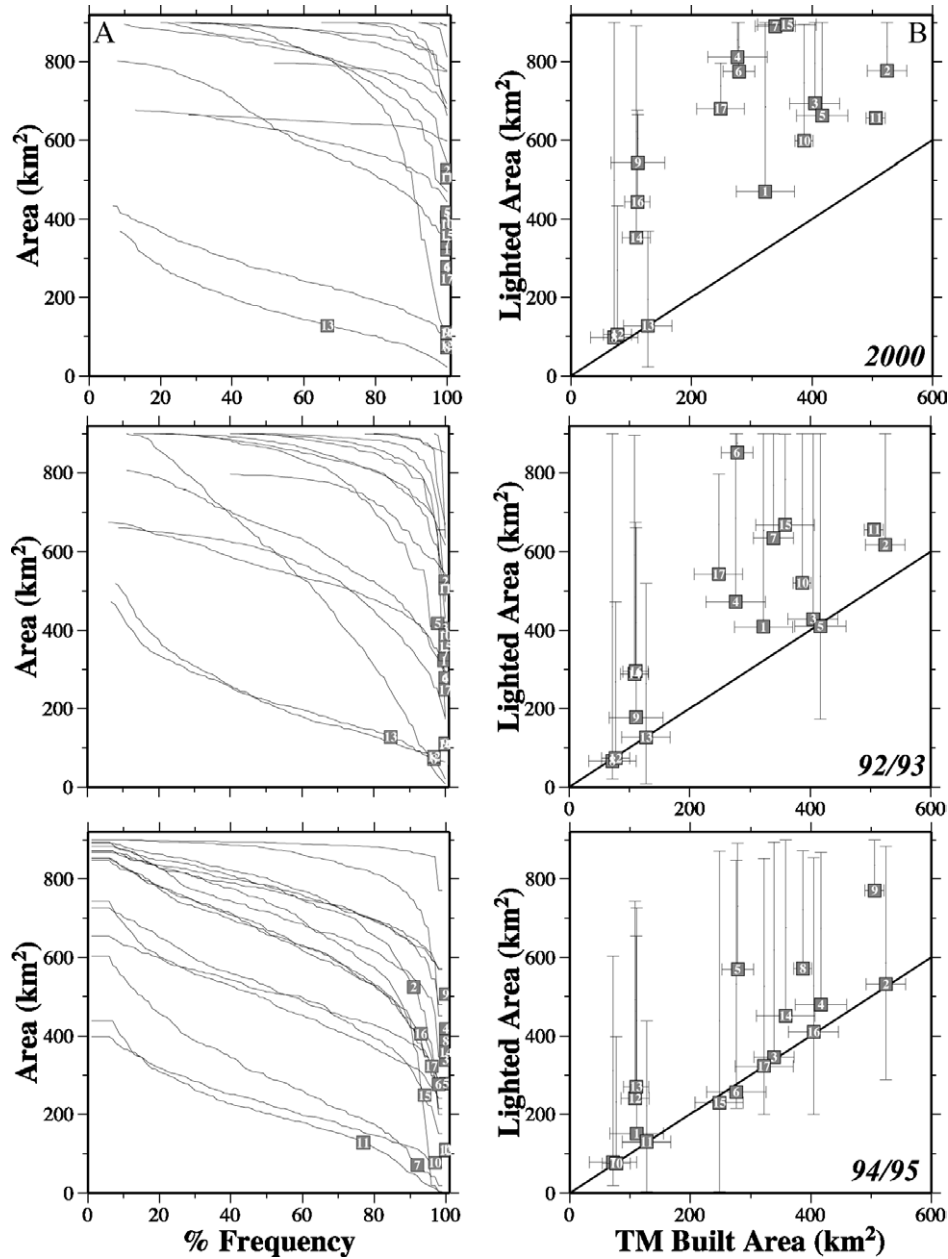


Fig. 8. Built and lighted areas for 17 cities. (A) Cumulative distribution curves on the left show the decrease in lighted area with increasing detection frequency threshold. Numbered squares (from Table 1) indicate the average built area from Landsat ETM+ imagery. In the 1994/1995 data, nine cities have built areas smaller than the area of $\geq 99\%$ frequency. In the 2000 data, only Pyongyang has a lighted area smaller than its built area while Hanoi and Port au Prince are only slightly smaller than the $\geq 99\%$ area. (B) Lighted areas of points near the 1:1 line correspond to optimal thresholds shown in A. Horizontal bars show the range of area estimates from ETM+ imagery and vertical bars show the range of areas between 1% and 100% lighted frequency.

Table 1

Number	City	Date
1	Beirut	6/22/00
2	Budapest	6/8/00
3	Cairo	8/23/00
4	Calcutta	11/15/00
5	Calgary	7/9/00
6	Guangzhou	9/14/00
7	Hanoi	12/20/01
8	Lagos	2/6/00
9	Miami	5/2/01
10	Port Au Prince	7/2/00
11	Pyongyang	5/6/01
12	San Salvador	12/31/99
13	Santo Domingo	9/22/00
14	Shanghai	6/14/01
15	St. Petersburg	4/25/00
16	Tianjin	3/6/00
17	Vienna	8/2/00

minimum lighted area (100% detection frequency) overestimates even the maximum built area estimate by several hundred km². One prominent exception is Pyongyang (13). In contrast, the 1994/1995 lighted areas more closely match the built area estimates at high detection frequencies (>90%). Although the 1994/1995 threshold lighted areas do sometimes correspond to the built areas, it is important to note that this correspondence does not occur at a consistent detection frequency threshold. In many cases the optimum threshold is >90% but in seven cases the 100% threshold is significantly smaller than the built area while in six cases, the 100% threshold is significantly larger than the built area. While 90% to 100% is a relatively narrow range of thresholds, it is the range where the lighted areas change most rapidly (see curves in Fig. 8) so a small difference in threshold results in a large difference (uncertainty) in the size of the lighted area.

The implication of this result is that there is not a single threshold that accurately estimates built area for any of the light datasets. However, this issue cannot be fully resolved from this type of analysis because of the fractal nature of the built area and the diffuse nature of urban lighting. Nonetheless, comparison of built areas in Fig. 7 and with the 1992/1993 and 2000 datasets confirms that lighted areas without thresholds always vastly overestimate maximal extents of built areas and that even 100% threshold areas usually overestimate built areas by a considerable margin in the 1992/1993 and 2000 datasets. Compared to administrative definitions of urban extent, physical estimates of built up area often provide an inherently conservative measure of urban extent because they do not include intraurban undeveloped area like parks and water bodies. However, physical estimates also eliminate the physically arbitrary boundaries that administrative definitions impose thereby providing a more consistent comparison of lighted area with the developed land cover that contains the source of the light. We attempt to circumvent this bias by using a range of built area estimates for each city. Comparisons of lighted area to urban extent provide an effective way to demonstrate the spatial correspondence between urban land cover and detectable light but the generally diffuse nature of the urban/rural gradient precludes direct estimation of blooming extent with most urban areas. For this reason, we consider urban development along coastlines.

5. Island comparison

To further quantify the spatial overextent of lighted area, we compared the 1994/1995 night lights dataset to the coastlines bounding several islands. Islands with coastal urban development provide an unambiguous boundary

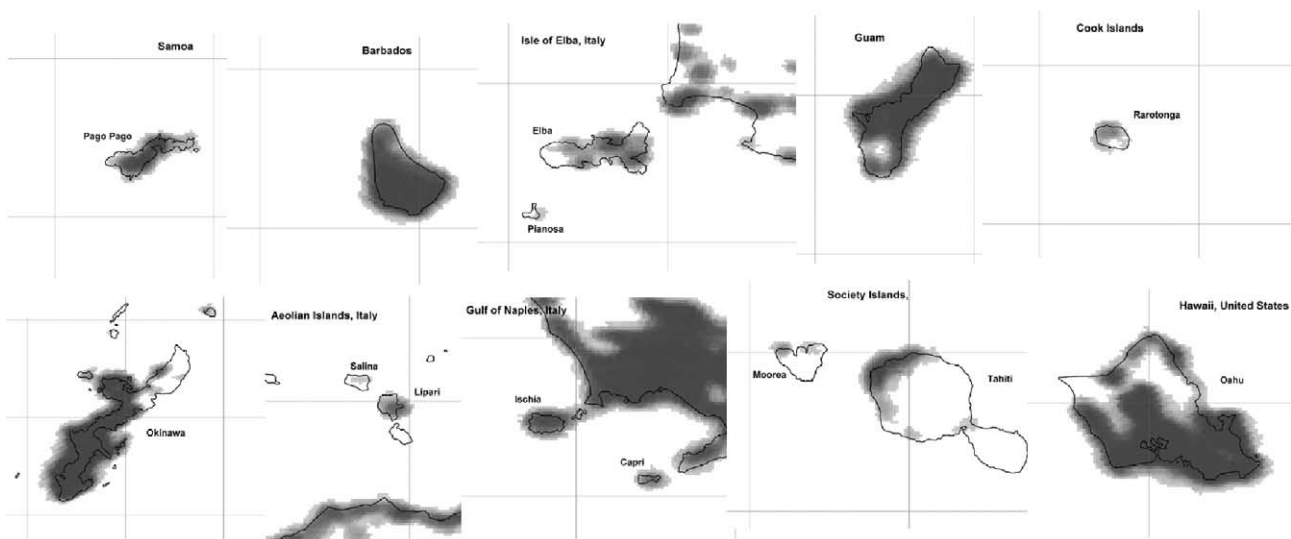


Fig. 9. Contiguously lighted islands in the 1994/1995 dataset. Superimposed coastlines highlight spatial extent of blooming over water. Darker gray indicates higher frequency of detection. Graticule interval is 0.5°.

between potentially lighted developed land and unlighted water. We selected islands rather than continental coastal cities because islands are generally convex and therefore provide a better estimate of radial extent of lighted area. In contrast, continental coastal cities are usually located around concavities in the coastline (like harbors and rivers) so the maximum distance of the lighted boundary from the coastline is more ambiguous. We did not compare the 1992/1993 and 2000 datasets because the previous analysis indicated that the spatial overextent in these datasets was consistently much greater than in the 1994/1995 dataset and because a land/sea mask was applied to these datasets during their production. The islands used in this analysis are shown in Fig. 9. The limiting constraint in selecting islands was the presence of lighted convex coastlines.

There appears to be a consistent relationship between contiguous lighted area and lateral extent of blooming for the islands investigated. Fig. 10 suggests a roughly linear relationship ($2 \times B = 0.25D + 2.7$) between lateral blooming and equivalent diameter for contiguous lighted areas smaller than 60 km diameter. We multiply the one-sided lateral extents of blooming by a factor of two for consistency with total diameter. While there is significant scatter in the relationship for the 10 islands we considered, the linear correlation of 0.89 is statistically significant and the least squares linear fit is generally consistent with the range of extents observed for 8 of the 10 islands. Rarotonga and Elba fall significantly below the trend. The blooming scale factor of 0.25 equivalent diameter implies a proportionality of 1.25 between built and lighted diameters for small, convex light

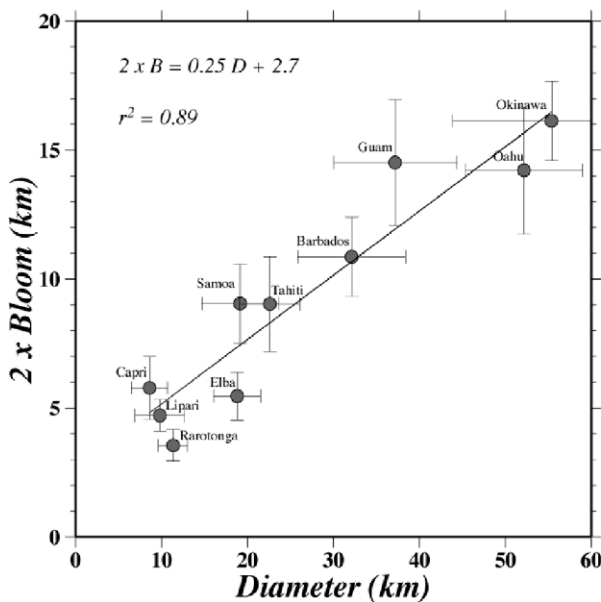


Fig. 10. Lateral extent of blooming for 10 islands in the 1994/1995 dataset. Average extent of blooming (circles) shows a quasi-linear increase with equivalent circular diameter ($2 \times 1D$ bloom) between ~ 10 and 60 km. Bars indicate the longitudinal and latitudinal maximum extents scaled to the diameter axis. Circles are averages of the maximum extents. The correlation is significant at 99%.

sources. A linear least squares fit to equivalent diameters of the built and lighted areas estimated by Elvidge et al. (2004) for 20 lighted settlements in California yields a proportionality of 1.21 and an intercept of 4.5. The consistency of the proportionality (1.25 and 1.21) and intercept (2.7 and 4.5) between two independent validation datasets and methodologies is encouraging. Moreover, the intercept of the island estimate (2.7 km) is consistent with the 2.2-km IFOV (at nadir) of the OLS sensor. We also investigated the correspondence between coastlines and % detection thresholds and found that no single threshold produced consistent agreement with the coastlines of the islands.

6. Discussion

The size–frequency distributions and their variation with % threshold reveal several important properties of the light datasets. The 14% threshold seen in the 1992/1993 and 2000 datasets may provide a useful cutoff to maximize the number of individual lights thereby balancing attenuation of small individual lights with reduction of spatial overextent around large cities. The size–frequency distributions in Fig. 3 indicate that increasing the threshold from 10% to 20% results in a sharp increase in the number of very small lights and that this secondary mode of the distribution persists as the threshold increases further. The appearance of this secondary mode suggests that much of the area observed at less than the 14% peak threshold is associated with interstitial blooming between settlements rather than individual small lights. The centroid frequency distributions in Fig. 4 support this assertion as they show that the distribution of individual lights peaks near the 14% threshold and drops rapidly at lower thresholds. Taken together, these observations suggest that most of the lighted pixels below the 14% threshold are associated not with small individual lights but with blooming on the periphery of larger settlements. The areas detected in less than 14% of observations correspond to 14% and 11% of the total areas of the 1992/1993 and 2000 datasets, respectively. Therefore, applying a 14% threshold significantly reduces blooming without attenuating many small settlements. In this sense, the 14% threshold provides the maximum information content for the 1992/1993 and 2000 datasets—although it still results in significant overestimation of individual city size. The analogous threshold in the 1994/1995 dataset occurs at 10% detection and corresponds to 15% of the total lighted area.

The consistency in the shape of the size–frequency distributions at different thresholds suggests that the distribution of individual lights is robust and may represent a fundamental property of the distribution of human settlements. As would be expected, increasing the threshold beyond 14% reduces the total number of lights and shifts the peak to slightly smaller sizes but it does not change the shape of the distribution. This implies that, as the threshold

increases, the attenuation of the smallest individual lights is balanced by the shrinkage of larger lights at a nearly equal rate to maintain the shape of the distribution. The rapidly diminishing number of lights with increasing size is consistent with well-known observations of rank-size rules for other measures of city size (e.g. Zipf's Rule). However, the nearly uniform distributions of area with diameter for ranges of 10 to almost 1000 km are not necessarily an obvious corollary to existing rank-size rules. To our knowledge, this is the first observation of a quasi-uniform total area–individual city size relationship at global scales. The fact that it persists over almost the entire range of thresholds suggests that it may be a true characteristic of the underlying city size distribution. The upward curvature of the Area/Perimeter distribution is also not dependent on the threshold which suggests that it too is a characteristic of the underlying spatial distribution of city shapes. As such, it could provide a simple but important constraint against which theoretical urban growth models and simulations could easily be tested.

The sigmoid distribution of diameter and detection frequency for individual lights smaller than ~ 10 km suggests that detection of small lights may be a Gaussian process that is dependent on city size. As equivalent diameter increases from 2 to 10 km, the modal detection frequency in Fig. 4 increases in a sigmoid manner suggestive of a Gaussian distribution. This is consistent with a random perturbation model for small settlement detection in which

$$P \sim \iint S(x,y) \delta(x,y) dx dy \quad (1)$$

where P is the probability of detection, $S(x,y)$ is the spatial sensitivity function given by the OLS sensor's Point Spread Function (PSF) and $\delta(x,y)$ is the presumably random spatial perturbation introduced by geolocation error. Sensor PSFs are often approximated by a 2D Gaussian function. If the geolocation error is also normally distributed then the Central Limit Theorem predicts that the convolution of these two Gaussian probabilities should also be Gaussian. Since individual small settlements are sparsely distributed within surrounding undeveloped (dark) areas, a Gaussian detection probability would result in a Gaussian detection frequency for a large number of imaging events. Thus the sigmoid variation of detection frequency with diameter for settlements approaching the dimension of the OLS sensor's Ground Instantaneous Field Of View (GIFOV) is consistent with the Gaussian probability described above. A detailed analysis is beyond the scope of the present study but we propose the detection model because knowing the detection probability of an individual small settlement would make it possible to estimate the true frequency distribution of settlements < 10 km. This would provide useful constraints for economic models of city size distribution.

In spite of the 14% threshold arguments made above, our results suggest that detection frequency thresholds do not provide a globally consistent basis for reconciling lighted

areas to urban extent. Both the city comparisons and the coastline comparisons highlight persistent inconsistencies in the relationship between threshold lighted area and urban extent. Given the number of factors influencing the extent and brightness of lighting and the probability of detection, this is not surprising. However, the quasi-linear relationships between lighted area and blooming extent shown in Fig. 10 and by Elvidge et al. (2004) may provide a basis for correcting the blooming problem. The consistency of our results with those of Elvidge et al. (2004) is encouraging but a more extensive analysis is needed. An analysis of convex lighted continental coastlines could provide a sufficient number of samples to test the linear assertion. From a physical standpoint, it is reasonable to expect larger settlements to be lighted more brightly and therefore to scatter more light into the atmosphere than smaller settlements. If this is the primary cause of blooming then we would also expect there to be a limit to the distance and intensity of this scattering. Geolocation error in the compositing process would also contribute to blooming but its spatial extent is not dependent on the size of the lighted area (above the apparent 10-km detection threshold) so this effect should be additive rather than multiplicative. This is consistent with the 2.7-km intercept predicted as settlement diameter approaches 0.

There were significant differences in the processing used to generate the 1994–1995 nighttime lights and the other two sets. The 1994–1995 dataset was percent frequency of cloud-free light detection—with no brightness information. The 1992–1993 and 2000 datasets have percent frequency of light detection plus the average digital number of the cloud-free light detections. The 1994–1995 set used the full orbital swath. The 1992–1993 and 2000 sets used only the center halves of the swaths. The lights are slightly smaller in the center halves, the geolocation is better, and the radiometry appears to be more consistent. Over the years, NGDC modified the algorithms to include more of the dim lighting—to detect more of the small towns and the “diffuse” lighting present in areas outside of cities and towns. This effort to detect more of the dim lighting was spurred on by users who reported findings such as “lighting was present for less than half the population of China”. The 1994–1995 set was processed as a stand alone product—not intended for change detection. The 1992–1993 and 2000 sets were specifically processed with all the same algorithms and setting to make the two sets as suitable for the detection of change in lighting as possible. The next sets, under construction now, will be even better for change detection.

Our results indicate that the 1994–1995 lights have better agreement with traditional boundaries of cities. The 1992–1993 and 2000 sets have light detected well beyond these traditional boundaries, due to the success in detection of dimmer lighting. The price paid for detecting the dimmer lights is the expansion of the blooming. It may be possible to model the blooming using radiance calibrated

nighttime lights as input into atmospheric models. Something like this was done several years ago, producing the first atlas of artificial sky brightness (Cinzano et al., 2001a,b). Alternatively, if the focus is on cities and towns, the peaks in Fig. 2 indicate that a significant amount of the blooming can be eliminated without losing many of the small settlements if the peaks are used to set local thresholds.

7. Conclusions

Previous studies of DMSP-OLS stable night lights have shown encouraging agreement between lighted areas and various definitions of urban extent. This suggests that night lights could provide a repeatable, globally consistent way to map size and spatial distributions of human settlements larger than some minimum detectable size or brightness. However, these studies have also highlighted an inconsistent relationship between the actual lighted area and the boundaries of the urban areas considered. Detection frequency thresholds can reduce the spatial overextent of lighted area (“blooming”) but thresholds also attenuate large numbers of smaller settlements and significantly reduce the information content of the night lights datasets. Quantitative spatial analysis of the widely used 1994/1995 stable lights data and the newly released 1992/1993 and 2000 stable lights datasets reveals the tradeoff between blooming and attenuation of smaller settlements. For the 1992/1993 and 2000 datasets, a 14% threshold significantly reduces blooming around large settlements without attenuating many individual small settlements. The corresponding threshold for the 1994/1995 dataset is 10%. The size–frequency distributions of each dataset retain consistent shapes for increasing thresholds while the size–area distributions suggest a quasi-uniform distribution of lighted area with individual settlement size between 10 and 1000 km equivalent diameter. Conurbations larger than 80 km diameter account for <1% of all settlements observed but account for about half the total lighted area worldwide. Area/perimeter distributions indicate that conurbations become increasingly dendritic as they grow larger.

Comparison of lighted area with built area estimates from Landsat imagery of 17 cities shows that lighted areas are consistently larger than even maximum estimates of built areas for almost all cities in every light dataset. Thresholds >90% can often reconcile lighted area with built area in the 1994/1995 dataset but there is not one threshold that works for a majority of the 17 cities considered. Even 100% thresholds significantly overestimate built area for the 1992/1993 and 2000 datasets. Comparison of lighted area with blooming extent for 10 lighted islands suggests a linear proportionality of 1.25 of lighted to built diameter and an additive bias of 2.7 km. This relationship is consistent with similar results obtained by Elvidge et al. (2004) for cities in

California. While more extensive analyses are needed, a linear relationship would be consistent with a physical model for atmospheric scattering combined with a random geolocation error. A Gaussian detection probability model is consistent with an observed sigmoid decrease of detection frequency for settlements <10 km diameter. Taken together, these observations could provide the basis for a scale-dependent blooming correction procedure that simultaneously reduces geolocation error and scattering induced blooming.

It is possible that the results could be improved by using the brightness of lighting as well as well as persistence (percent frequency of detection) used in this study. The OLS is not well suited for deriving calibrated radiances due to a lack of on-board calibration and saturation of lights in urban centers for most of the OLS archive. A new generation of annual global OLS nighttime lights is currently in production for the 1992–2003 time period. The new products will report the average visible band digital numbers (DN) of lights, but will not be radiometrically calibrated. NGDC plans to cross calibrate each of the annual products, but in relative sense, not absolute. The Visible Infrared Imaging Radiometer Suite (VIIRS) instrument will continue the low light imaging measurements of the OLS, with substantial improvements in calibration, spatial resolution and levels of quantization. It is anticipated that the nighttime lights products derived from VIIRS data will be superior to those possible from the OLS.

References

- Balk, D., Pozzi, F., Yetman, G., Nelson, A., & Deichmann, U. (2004). What can we say about urban extents? Methodologies to improve global population estimates in urban and rural areas? *Population association of America annual meeting, Boston, MA*.
- Batty, M., & Longley, P. (1996). *Fractal Cities*. London and San Diego: Academic Press. 394 p.
- Cincotta, R. P., Wisniewski, J., & Engelman, R. (2000). Human population in the biodiversity hotspots. *Nature*, 404, 990–992.
- Cinzano, P., Falchi, F., & Elvidge, C. D. (2001a). The first world atlas of the artificial night sky brightness. *Monthly Notices of the Royal Astronomical Society*, 328, 689–707.
- Cinzano, P., Falchi, F., Elvidge, C. D., & Baugh, K. E. (2001b). The artificial sky brightness in Europe derived from DMSP satellite data. *Preserving the astronomical sky* (pp. 95–102).
- Croft, T. A. (1978). Nighttime images of the earth from space. *Scientific American*, 239, 86–89.
- Elvidge, C. D., Baugh, K. E., Kihn, E. A., Kroehl, H. W., Davis, E. R., & Davis, C. W. (1997). Relation between satellite observed visible–near infrared emissions, population, economic activity and electric power consumption. *International Journal of Remote Sensing*, 18(6), 1373–1379.
- Elvidge, C. D., Safran, J., Nelson, I. L., Tuttle, B. T., Hobson, V. R., Baugh, K. E., et al. (2004). Area and position accuracy of DMSP nighttime lights data. *Remote sensing and GIS accuracy assessment* (pp. 281–292). CRC Press.
- Fujita, M., Krugman, P., & Mori, T. (1999). On the evolution of hierarchical urban systems. *European Economic Review*, 43(2), 209–251.

- Henderson, M., Yeh, E. T., Gong, P., Elvidge, C., & Baugh, K. (2003). Validation of urban boundaries derived from global night-time satellite imagery. *International Journal of Remote Sensing*, 24(3), 595–609.
- Imhoff, M. L., Lawrence, W. T., Stutzer, D. C., & Elvidge, C. D. (1997). A technique for using composite DMSP/OLS “city lights” satellite data to map urban area. *Remote Sensing of Environment*, 61(3), 361–370.
- Krugman, P. (1996). Confronting the mystery of urban hierarchy. *Journal of the Japanese and International Economies*, 10(4), 399–418.
- Small, C. (2002). A global analysis of urban reflectance. In D.M.a.F.S.-E.C. Jurgens (Ed.), *Proceedings of the Third International Symposium on Remote Sensing of Urban Areas*. Istanbul, Turkey.
- Small, C. (2003). High spatial resolution spectral mixture analysis of urban reflectance. *Remote Sensing of Environment*, 88(1–2), 170–186.
- Small, C. (2005). A global analysis of urban reflectance. *International Journal of Remote Sensing*, 26(4), 661–681.
- Sutton, P., Roberts, C., Elvidge, C., & Meij, H. (1997). A comparison of nighttime satellite imagery and population density for the continental united states. *Photogrammetric Engineering and Remote Sensing*, 63(11), 1303–1313.
- Sutton, P., Roberts, D., Elvidge, C., & Baugh, K. (2001). Census from Heaven: An estimate of the global human population using night-time satellite imagery. *International Journal of Remote Sensing*, 22(16), 3061–3076.
- Welch, R. (1980). Monitoring urban-population and energy-utilization patterns from satellite data. *Remote Sensing of Environment*, 9(1), 1–9.
- Welch, R., & Zupko, S. (1980). Urbanized area energy-utilization patterns from Dmsp data. *Photogrammetric Engineering and Remote Sensing*, 46(2), 201–207.